PERGAMON

International Journal of Heat and Mass Transfer 44 (2001) 1475–1484

International Journal of HEAT and MASS TRANSFER

www.elsevier.com/locate/ijhmt

Forced convective boiling of binary mixtures in annular flow. Part II: heat and mass transfer

J.R. Barbosa Jr., G.F. Hewitt *

Department of Chemical Engineering and Chemical Technology, Imperial College of Science, Technology and Medicine, London SW7 2BY, UK

Received 5 November 1999; received in revised form 20 June 2000

Abstract

The present paper proposes a model for phase change heat transfer to binary mixtures at high qualities (annular flow regime). Use is made of a Colburn–Drew type formulation for calculation of interfacial parameters (mass fluxes, compositions and temperature). It is observed that, when combined with the hydrodynamic effects due to droplet interchange described in Part I, the formulation gives a very good prediction of bulk and wall temperatures and the deterioration in the heat transfer coefficient reported by Kandlbinder [Experimental investigation of forced convective boiling of hydrocarbons and hydrocarbon mixtures, Ph.D. thesis, University of London, Imperial College, 1997] for forced convective boiling experiments in a vertical, electrically heated, stainless steel, 25.4 mm ID test section using binary hydrocarbon mixtures.

1. Introduction

This is the second part of a paper devoted to the description of forced convective boiling of binary mixtures at high qualities. Here, a model for simultaneous interphase heat and mass transfer is developed so as to explain the different trends of variation of heat transfer coefficient observed by Kandlbinder [1]; in Kandlbinder's experiments, it was found that (in forced convective evaporation) the heat transfer coefficient could decrease with increasing quality, contradicting what is expected for single component fluids, i.e., increasing heat transfer coefficient trends with increasing quality. The proposed methodology is based on a Colburn–Drew formulation and incorporates the combined effect of droplet interchange (entrainment and deposition) described in Part I of this paper.

In what follows, Section 2 gives a brief overview of the predictive methods for forced convective boiling of mixtures available in the literature. Section 3 describes the modelling of interphase heat and mass transfer carried out in the present work. Results are shown in Section 4. Predictions of local heat transfer coefficients and of wall, interface and core temperatures are presented and compared with the experimental results by Kandlbinder [1] for boiling of *n*-pentane/iso-octane mixtures in a vertical, 25.4 mm ID, 8.68 m long, electrically heated, stainless steel test section. Finally, conclusions are drawn in Section 5.

2. Review of prediction methods for convective boiling of mixtures

Predictive methods for boiling of single component fluids form the basis for development of methods for mixtures. The most widely used correlation for this case is the one proposed by Chen [2]. Chen postulates that the heat transfer coefficient is made up of two parts: (a) a micro-convective (or nucleate boiling) portion α_{mic}, and, (b) a macro-convective (or forced convective) portion, α_{mac},

$$\alpha = \alpha_{mac}F + \alpha_{mic}S, \tag{1}$$

where

$$\alpha_{mac} = 0.023\frac{\lambda_L}{d_T}Re_L^{0.8}Pr_L^{0.4}, \tag{2}$$

* Corresponding author.

0017-9310/01/$ - see front matter
PII: S0017-9310(00)00210-6

Nomenclature

C_{mix}	mixture correction factor
c_p	specific heat capacity at constant pressure (J kg^{-1} K^{-1})
d_T	diameter of tube (m)
D	deposition rate (kg m^{-2} s^{-1})
E	entrainment rate (kg m^{-2} s^{-1})
F	enhancement factor in Chen correlation
$\dot{m}$	mass flux (kg m^{-2} s^{-1})
p	pressure Pa
Pr	Prandtl number
$\dot{q}$	heat flux (W m^{-2})
Re	Reynolds number
s	thickness of layer (film method) (m)
S	suppression factor in Chen correlation
T	temperature (K)
x	composition of liquid (mass fraction)
X	quality
X_{tt}	Martinelli parameter
y	composition of vapour (mass fraction)
y	auxiliar radial co-ordinate (m)
z	axial co-ordinate (m)

Greek symbols

α	heat transfer coefficient (W m^{-2} K^{-1})
β_{12}	mass transfer coefficient (m s^{-1})
Δ_{12}	mass diffusivity (m^2 s^{-1})
Δh_v	latent heat of vaporisation (J kg^{-1})
ΔT_{bp}	boiling range (K)
λ	thermal conductivity (W m^{-1} K^{-1})
η	viscosity (N s m^{-2})
ϕ	finite flux correction factor for mass transfer
ϕ_T	finite flux correction factor for heat transfer
ρ	density (kg m^{-3})
σ	surface tension N m^{-1}

Subscripts

b	bulk
C	core
E	equilibrium
GC	vapour/gas in the core
i	component identifier, 1-pentane
I	interface
L	liquid phase
LE	entrained liquid
LF	liquid film
mac	macro-convective
mic	micro-convective
sat	saturation
tp	two-phase
w	wall

Superscript

•	finite flux

$$Re_L = \frac{\dot{m}_L d_T}{\eta_L}, \tag{3}$$

$$Pr_L = \frac{\eta_L c_{pL}}{\lambda_L}, \tag{4}$$

$$F = \begin{cases} 1 & \text{if } \frac{1}{X_{tt}} > 0.1, \\ 2.35\left[\frac{1}{X_{tt}} + 0.213\right]^{0.736} & \text{if } \frac{1}{X_{tt}} \leqslant 0.1, \end{cases} \tag{5}$$

$$\frac{1}{X_{tt}} = \left(\frac{\rho_L}{\rho_G}\right)^{0.5}\left(\frac{\eta_G}{\eta_L}\right)^{0.1}\left(\frac{X}{1-X}\right)^{0.9}, \tag{6}$$

$$\alpha_{mic} = 0.00122\frac{\lambda_L^{0.79} c_{pL}^{0.45} \rho_L^{0.49} \Delta T_{sat}^{0.24} \Delta p_{sat}^{0.75}}{\sigma^{0.5} \eta_L^{0.29} \rho_G^{0.24} \Delta h_V}, \tag{7}$$

$$S = \frac{1}{1 + 2.53 \times 10^{-6} Re_{tp}^{1.17}}, \tag{8}$$

$$\Delta T_{sat} = T_w - T_{sat}, \tag{9}$$

$$\Delta p_{sat} = p_{sat}(T_w) - p_{sat}(T_{sat}) \tag{10}$$

and,

$$Re_{tp} = Re_L F^{1.25}. \tag{11}$$

The original paper gave graphical correlations for F and S; Eqs. (5) and (8) are later empirical fits to the graphical relationships. An adaptation of the Chen correlation for mixtures was proposed by Bennett and Chen [3], based on data obtained with an ethylene glycol–water mixture. Modified enhancement and suppression factors were proposed so as to cope with mixture effects in both micro- and macro-convective portions. Celata et al. [4] compared both the Chen [2] and the Bennett and Chen [3] correlations with their data for boiling of refrigerant mixtures. They found that the performance of the correlation for single component fluids was very similar to that for mixtures. The Chen [2] correlation showed only a slightly larger scatter than the Bennett and Chen [3] correlation with most of their data lying within an error band greater than ±20%. The correlation by Mishra et al. [5] was also implemented, but it showed lower accuracy.

Palen [6] also suggested the use of a modified form of the correlation by Chen [2] for boiling of mixtures. In this case, the nucleate boiling coefficient was adjusted for

mixture effects but no correction was proposed for the forced convective contribution.

The heat transfer coefficient is given by

$$\alpha = \alpha_{mac}F + \alpha_{mic}C_{mix}S, \tag{12}$$

where C_{mix} is a mixture correction factor defined by Palen and Small [7] as,

$$C_{mix} = \exp(-0.027\Delta T_{bp}), \tag{13}$$

where ΔT_{bp} is the boiling range (difference between the dew point and bubble point temperatures).

Kandlbinder [1], after comparing the performance of several correlations for boiling of mixtures, concluded that, though none of the existing correlations performed well, the correlation by Chen [2] with correction suggested by Palen [6] gave the best results. Thus, the Chen/Palen formulation was chosen for the calculation of wall temperatures carried out in the present paper. Such a calculation is part of a complete methodology fully described in the next section. More recently, Kandlikar [8] proposed an upgraded correlation for binary systems based on a correlation for pure fluids [9]. This incorporates the diffusion-induced nucleate boiling suppression factor to account for severe suppressions observed for mixtures with larger volatility differences.

In forced convective evaporation of binary mixtures in annular flow, the interface concentration of each component will normally be different from their concentrations in the bulk vapour. The interface concentrations must be such as to allow the diffusion of the evaporating material from the interface into the bulk. This leads to a mass transfer resistance effect analogous to that found in condensation. Thus, whereas in condensation of multicomponent mixtures, the interface temperature is *reduced* relative to the equilibrium value, the interface temperature in evaporation is *increased* relative to the equilibrium value. Two main types of methods have been used for estimating these mass transfer effects. The first class of methods is based on the approximate methods for condensation developed by Silver [10] and Bell and Ghaly [11] (the SBG methods); the studies of Palen et al. [12], Sardesai et al. [13] and Murata and Hashizume [14] fall into this category. A more refined class of models are those based on the Colburn film theory. Shock [15] investigated theoretically the purely convective region by writing balances for the components over an element as the sum of diffusive and net flow portions. Closure relationships for heat and mass transfer on the vapour side were given by the Chilton–Colburn analogy. In the liquid film, mass transfer was calculated via an extension of the method of Hewitt [16] for heat transfer in single component flows. The model was applied to water–ethanol mixtures and, as the main conclusion, it can be said that the role of mass transfer resistance within the phases was found to be not very important in the cases studied. However, Thome and Shock [17] pointed out that such conclusions may not be valid for systems with wider boiling ranges (as the hydrocarbon mixtures studied here). In addition, the effects due to droplet interchange and interfacial roughness were not assessed by Shock's formulation.

3. Modelling

3.1. The heat transfer coefficient

In order to validate the analysis presented in this paper, comparisons with experimental data have been carred out in two different ways: (i) comparison of predicted and measured wall temperatures: (ii) comparison of heat transfer coefficients. The heat transfer coefficient in multicomponent mixtures is normally defined by the following equation:

$$\alpha = \frac{\dot{q}_w}{(T_w - T_E)}, \tag{14}$$

where T_E is the flow equilibrium bulk temperature calculated from the local mean enthalpy and pressure. As a result of the postulated existence of different compositions in the film and in the droplets, α as defined by Eq. (14) will be different from α as defined by the ratio of the heat flux to the temperature difference across the film. However, since the wall temperature, T_w, is calculated as part of the present methodology, since T_E can also be estimated using the vapour–liquid equilibrium routines and since $\dot{q}_w$ is known, it will be possible to obtain a *predicted* heat transfer coefficient from Eq. (14) which can be compared with the *experimental* heat transfer coefficient calculated from Eq. (14) using the *measured* values of T_w.

The wall temperature is calculated by applying to the interface temperature the Chen [2] correlation with the (small) nucleate boiling component corrected for multicomponent effects [6]. T_I, in turn, is obtained as part of a solution of a system of equations for interphase heat and mass transfer. This system is modelled via a Colburn–Drew methodology and is the subject of the next section.

3.2. Interphase heat and mass transfer

As mentioned in Section 1, a methodology analogous to that of condensation problems is pursued here. Though, for completeness, a summary of the methodology is given here, the reader who wishes to have a more detailed description is referred to the papers of Webb and McNaught [18] and Webb [19].

The physics of the problem is schematically illustrated in Fig. 1. It is postulated that the annular flow regime prevails and liquid is present in the core in the form of small entrained droplets. Droplet interchange

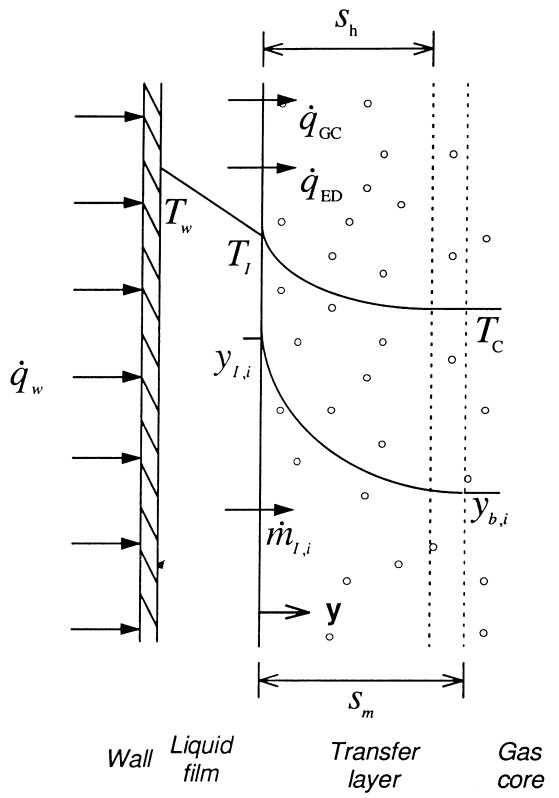

Fig. 1. Illustration of the problem.

between the core and the liquid film occurs as described in Part I of this paper. The gas phase is a saturated or a subcooled mixture which may contain non-condensing gases as well as vapours. All the resistances to heat and mass transfer in the gas side are assumed to lie in thin layers of thicknesses s_h and s_m adjacent to the interface. The flow in such layers is assumed to be steady, laminar, and one-dimensional. Transport properties are considered constant. Homogeneous chemical reactions, viscous dissipation, and radiant-emission or absorption in the fluid are neglected.

Energy is transferred to the vapour flowing in the core in the form of latent and sensible heat

$$\dot{q}_{GC} = \dot{q}_{GC,L} + \dot{q}_{GC,S}. \tag{15}$$

Latent energy is released due to evaporation taking place at the interface. It is given by

$$\dot{q}_{GC,L} = \sum_{i=1}^{2} \dot{m}_{I,i} \Delta h_{v,i}. \tag{16}$$

The release of sensible energy to the vapour is due to two distinct mechanisms: (i) cooling of the evaporating component from T_I to T_C (the mean temperature of the homogeneous core) as it travels from the interface to the bulk and, (ii) heating of the vapour in the core from T_C to $(T_C + \Delta T_C)$ (conduction of heat through the laminar layer). These are as follows:

$$\dot{q}_{GC,S} = \sum_{i=1}^{2} \dot{m}_{I,i} c_{pGC,i} (T - T_C) - \lambda \frac{dT}{d\mathbf{y}}. \tag{17}$$

Integrating from $\mathbf{y} = 0$ to $\mathbf{y} = s_h$, with the boundary conditions shown in Fig. 1, gives

$$\dot{q}_{GC,S} = \alpha^{\bullet}_{GC} e^{\phi_T} (T_I - T_C), \tag{18}$$

where

$$\alpha^{\bullet}_{GC} = \frac{\alpha_{GC} \phi_T}{e^{\phi_T} - 1}, \tag{19}$$

$$\alpha_{GC} = \frac{\lambda_{GC}}{s_h} \tag{20}$$

and

$$\phi_T = \frac{1}{\alpha_{GC}} \sum_{i=1}^{2} \dot{m}_{I,i} c_{pGC,i}. \tag{21}$$

The total energy to the vapour in the core is thus,

$$\dot{q}_{GC} = \sum_{i=1}^{2} \dot{m}_{I,i} \Delta h_{v,i} + \alpha^{\bullet}_{GC} e^{\phi_T} (T_I - T_C). \tag{22}$$

With the above simplifying assumptions and using Fick's Law as the constitutive relationship for the diffusive mass fluxes, the equations of change for the vapour mass fluxes in the layer are [20]

$$\frac{d}{d\mathbf{y}} \left[y_i \sum_{i=1}^{2} \dot{m}_i - \rho_{GC} \Delta_{12} \frac{d}{d\mathbf{y}} y_i \right] = 0. \tag{23}$$

Integration over the limits $\mathbf{y} = 0$ and $\mathbf{y} = s_m$ with the appropriate boundary conditions gives,

$$\dot{m}_I = \rho_{GC} \beta^{\bullet}_{12} \left(\frac{y_{I,1} - y_{b,1}}{z - y_{I,1}} \right), \tag{24}$$

where

$$\dot{m}_I = \dot{m}_{I,1} + \dot{m}_{I,2}, \tag{25}$$

$$z = \frac{\dot{m}_{I,1}}{\dot{m}_I}, \tag{26}$$

$$\beta^{\bullet}_{12} = \beta_{12} \frac{\phi}{(e^{\phi} - 1)} \tag{27}$$

and

$$\phi = \frac{\dot{m}_I}{\rho_{GC} \beta_{12}}. \tag{28}$$

Eq. (24) is not a complete description of the evaporation process as only it diffusional part was specified. Another relationship is needed (determinacy condition) so that $\dot{m}_I$

is known. Two kinds of determinacy conditions may be used; as in condensation, they are linked to degree of mixing in the liquid film (condensate). The first determinacy conditions – *fully mixed liquid film* – is appropriate for vertical tubes where the liquid film flow is turbulent. It is assumed that no radial gradients of concentration exist in the film. Thus, $x_{LF_{I,1}} = x_{LF_{b,1}} = (\dot{m}_{I,1})/\dot{m}_I$. The second determinacy condition – *unmixed liquid film* – is typical of laminar liquid film flow in vertical tubes and of horizontal geometries. For this condition, $x_{LF_{I,1}} = (\dot{m}_{I,1})/\dot{m}_I$. It is expected that real cases lie between these two extremes. For the present geometry and flow regime in the liquid film, the first determinacy condition – *fully mixed liquid* – seems more appropriate (the action of disturbance waves is towards a homogenisation of the concentration in the film). In this case, the interfacial liquid composition is known a priori (previous liquid film evaporation) and a bubble point calculation defines the interfacial state (vapour composition and interfacial temperature).

An energy balance over an element of the homogeneous core of length dz (see Fig. 1) gives,

$$\dot{m}_C c_{pC} \frac{d}{dz} T_C = \frac{4}{d_T}[\alpha^{\bullet}_{GC}(T_I - T_C) + (E - \langle D \rangle) c_{pLE}(T_I - T_C)], \tag{29}$$

where the first term in the RHS is the conductive contribution of the heat flux to the vapour-phase. The second term in the RHS is the net energy released/absorbed by the entrained liquid due to entrainment and deposition. $\dot{m}_C, c_{pC}$ and T_C are the homogeneous core mass flux, specific heat capacity and temperature, respectively. These are given by:

$$\dot{m}_C = \dot{m}_{GC} + \langle \dot{m}_{LE} \rangle, \tag{30}$$

$$c_{pC} = \frac{\dot{m}_{GC} + \langle \dot{m}_{LE} \rangle}{\dot{m}_{GC}/c_{pGC} + \langle \dot{m}_{LE}/c_{pLE} \rangle}, \tag{31}$$

$$T_C = \frac{\dot{m}_{GC} c_{pGC} + \langle \dot{m}_{LE} c_{pLE} \rangle}{\dot{m}_{GC} c_{pGC}/T_{GC} + \langle \dot{m}_{LE} c_{pLE}/T_{LE} \rangle}, \tag{32}$$

where the cumulative operator $\langle\,\rangle$ is defined as in part I.

An additional closure hypothesis is as follows:

$$\dot{q}_{GC} = \dot{q}_w - \dot{q}_{ED}, \tag{33}$$

where

$$\dot{q}_{ED} = (E - \langle D \rangle) c_{pLE}(T_I - T_C). \tag{34}$$

This assumption states that the wall heat flux is equal to the sum of the energy absorbed by the vapour and that absorbed by the entrained droplets due to entrainment and deposition.

A conservation equation for the bulk vapour concentration is as follows:

$$\frac{d}{dz} y_{b,i} = \frac{4}{d_T \dot{m}_{GC}} (\dot{m}_{I,i} - \dot{m}_I y_{b,i}). \tag{35}$$

Eqs. (29) and (35) are solved, together with the overall mass and momentum and film component mass balance equations derived in Part I, within a marching algorithm for the annular flow region. At each step dz, an iterative procedure is carried out to determine the interfacial mass fluxes, compositions and temperature. The solution algorithm comprises the following steps:

1. known: $x_{LF_{I,1}} (= x_{LF_{b,1}}), y_{b,1}, T_C$;
2. calculate $y_{I,1}, T_I \rightarrow$ bubble point temperature subroutine;
3. guess: $\dot{m}_I$;
4. calculate $z\ (= \dot{m}_{I,1}/\dot{m}_I) \rightarrow$ Eq. (24);
5. calculate: $\dot{q}_{GC} \rightarrow$ Eq. (22);
6. compare: If $\dot{q}_{GC} \neq \dot{q}_w - \dot{q}_{ED}$, update $\dot{m}_I$ and return to step 4.

The gas-phase heat and mass transfer coefficients are calculated via Dittus–Boelter type relationships. As suggested by Webb et al. [21], no enhancement due to interfacial wave effects or entrainment was taken into account in such a calculation. The vapour side mass diffusivities are calculated via the method by Fuller et al. [22]. Other physical properties are estimated by the same methods described in Part I.

Finally, wall temperatures are determined using the calculated interface temperature, the wall heat flux and the heat transfer coefficient obtained via the Chen/Palen formulation. As already mentioned in Part I, there is at present no general method for calculating the entrained fraction at the onset of annular flow. Thus, the approach of assuming a series of values covering the likely range (i.e., 0%, 10%, 20% and 40%) and carrying out calculations for each of these values is still undertaken in the heat and mass transfer calculations.

4. Results

In the present section, the heat transfer results are compared with the experimental data obtained by Kandlbinder [1] for binary (*n*-pentane/iso-octane) mixtures. In Kandlbinder's experiments, thermocouples were located at the outer wall and at the centreline of the tube. In order to estimate the inner wall temperatures (values with which the present predictions are compared), Kandlbinder solved the heat conduction equation with internal heat generation, having the outer wall temperatures as boundary conditions. As far as the bulk temperature measurements are concerned, it is expected that, due to the distribution of the phases in the annular flow pattern (the thickness of the liquid film is of the order of a fraction of millimeter), the temperature profiles recorded by the bulk (centreline) thermocouples are

Table 1
Summary of condition in calculations

Run No.	$\tilde{x}_{ov}$	p (MPa)	$\dot{q}_w$ (kW m^{-2})	$\dot{m}_T$ (kg m^{-2} s^{-1})
Run 1	0.7/0.3	0.23	57.7	286.6
Run 2	0.7/0.3	0.30	59.6	303.1
Run 3	0.7/0.3	0.60	60.2	295.0
Run 4	0.7/0.3	0.23	49.8	292.8
Run 5	0.7/0.3	0.61	68.4	503.8
Run 6	0.7/0.3	0.32	49.3	305.0
Run 7	0.7/0.3	1.00	49.8	299.2
Run 8	0.35/0.65	0.22	59.4	295.2
Run 9	0.35/0.65	0.29	58.9	302.2
Run 10	0.35/0.65	0.61	59.1	304.9
Run 11	0.35/0.65	0.22	40.7	195.8
Run 12	0.35/0.65	0.22	49.3	297.1

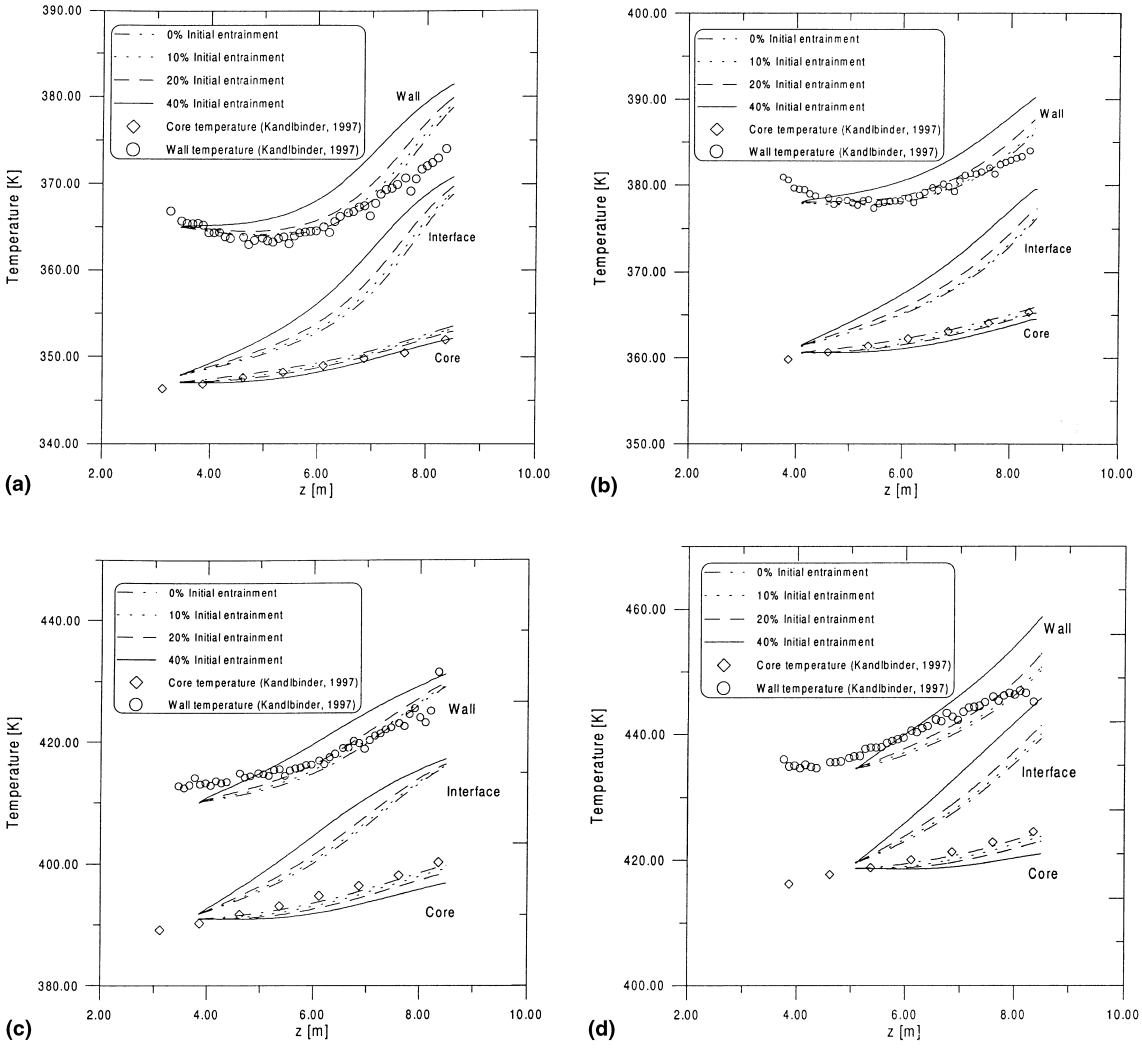

Fig. 2. Predictions of wall, interface and core temperatures: (a) Run 4, (b) Run 6, (c) Run 3, (d) Run 7. Conditions are those of Table 1.

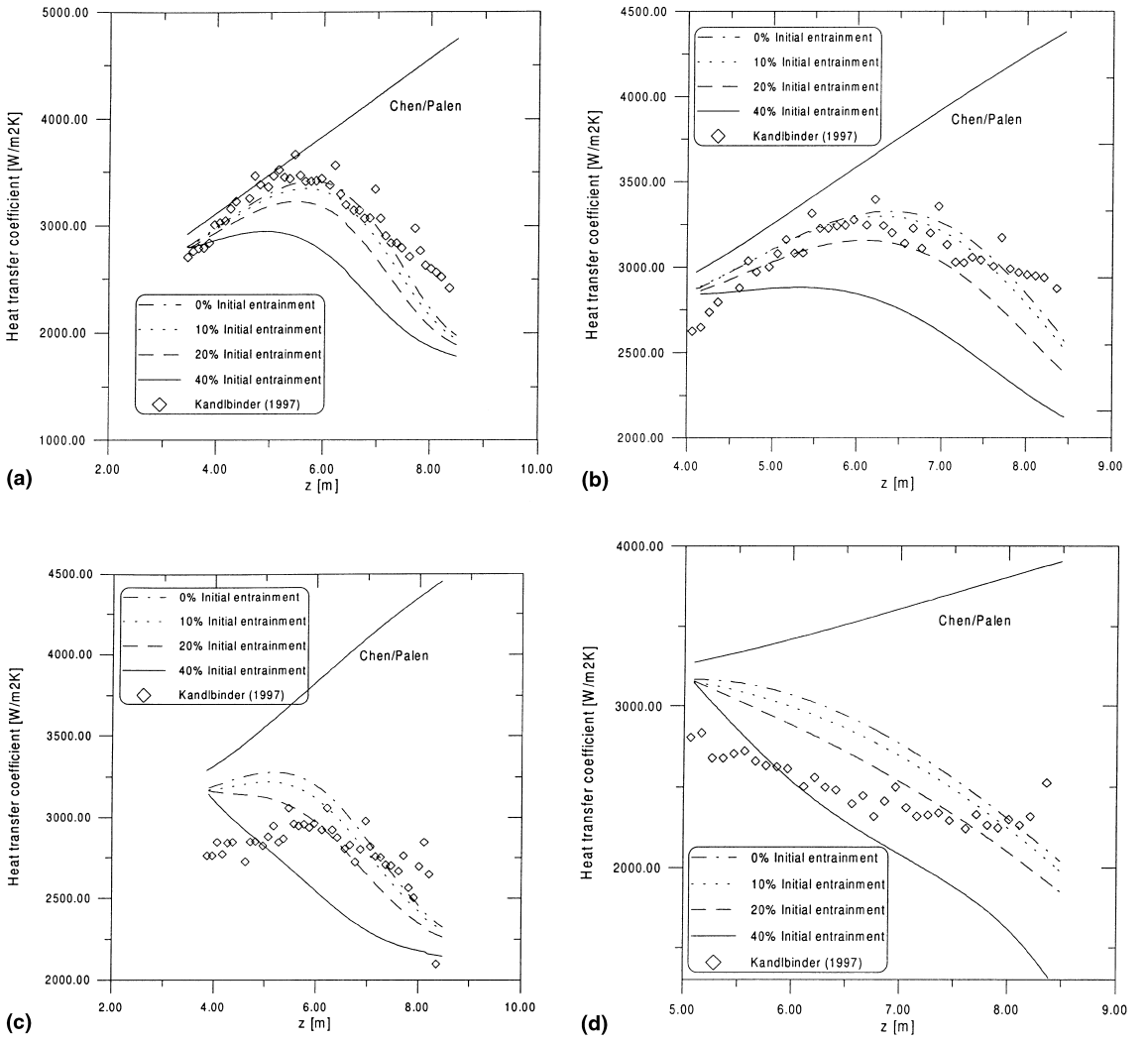

Fig. 3. Predictions of heat transfer coefficient: (a) Run 4, (b) Run 6, (c) Run 3, (d) Run 7. Conditions are those of Table 1.

those corresponding to the homogeneous core. Thus, the predicted distributions of T_C are compared with the experimental data.

The conditions in the calculations are the same as presented in Part I and are shown in Table 1 for completeness. Fig. 2(a)–(d) show the predictions of wall, interface and core temperatures for different initial entrained fractions at various conditions. As for the distributions of mean concentration in the film and in the entrained droplets, a variation in the initial entrained fraction provokes an opposite effect in the behaviour of mean temperatures; higher values of initial $\dot{m}_{LE}$ induce lower profiles of T_C and higher profiles of T_i. It can be observed that the measured temperature trends are well picked up by the formulation, but the agreement somewhat decreases with increasing pressure. The probable reason for the discrepancy between the present model and the data at higher pressures is that the various correlations and methods embodied in the proposed formulation were originally obtained from low-pressure data.

The measured heat transfer coefficients, calculated by introducing the known wall heat flux, the measured wall temperature and the calculated value of T_E into Eq. (14), are compared with those calculated using the present methodology in Fig. 3(a)–(d) for the same conditions as in Fig. 2. Again, the capability of the formulation at predicting the decrease in the heat transfer coefficient with increasing quality is evident.

Also shown in Fig. 3(a)–(d) are the predictions obtained from the Chen [2] correlation taking account of mixture effects on the (small) nucleate boiling coefficient using the correlation of Palen and Small [7]. As will be seen, this modified version of the Chen correlation overpredicts the heat transfer coefficients.

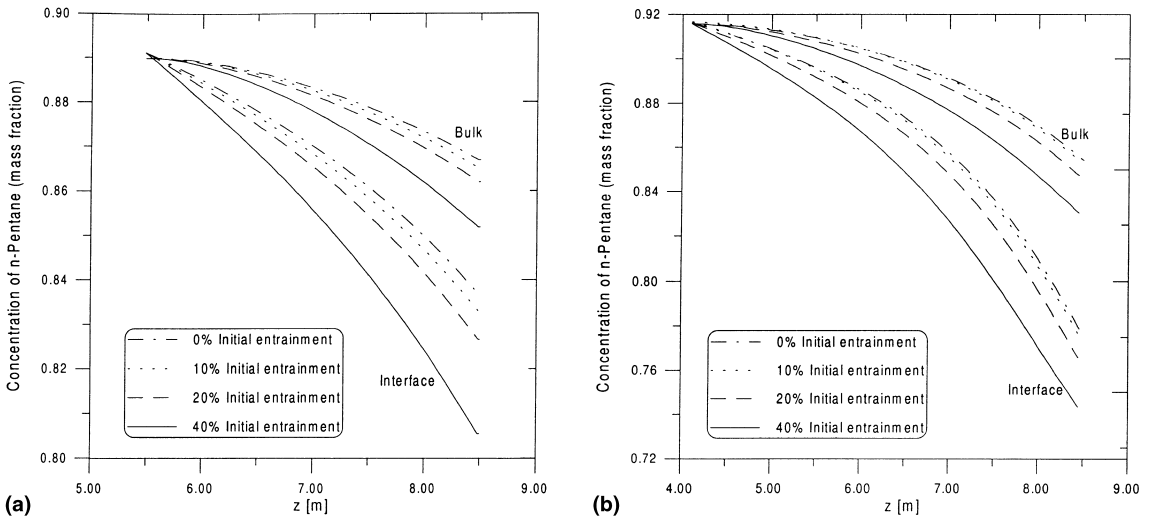

Fig. 4. Profiles of bulk and interfacial concentrations of *n*-pentane in the vapour core: (a) Run 5, (b) Run 6. Conditions are those of Table 1.

Since the Chen/Palen method was also used in the present methodology for calculating the film coefficient, the difference between the Chen/Palen predictions based on a conventional interpretation and those arising from the present model (combined effect of droplet interchange and mass transfer resistance) give a direct indication of the importance of these mechanisms. As observed, a very significant effect is predicted.

As mentioned before, there is at present no method for calculating the initial entrained fraction and it is expected that such a value is higher than that obtained by equating the entrainment and deposition rates (equilibrium value) at the point of onset of annular flow. An analysis of Figs. 2 and 3 suggests that the likely value of the initial entrained fraction for the cases studied lies in the 10–20% range (higher than the 5–10% equilibrium values range).

In Fig. 4(a) and (b), typical profiles of bulk and interfacial vapour concentrations are presented for various initial entrained fractions. As expected, an increase in the initial entrained fraction gives lower predictions of $y_{b,1}$ and $y_{I,1}$, as a lower amount of liquid is available in the film for evaporation. Surprisingly, profiles of interface concentration are lower than those for the bulk vapour. This trend (expected for condensation) was also observed in the simulation of Shock [15].

Fig. 5(a) and (b) show typical plots of the ratio $\dot{q}_{ED}/\dot{q}_w$ against the axial distance. It is observed that the energy absorbed/released by the entrained droplets due to droplet interchange is lower than 10% of the wall heat flux. Moreover, as the liquid film gets thinner (due to entrainment and phase change), the entrainment rate decreases and the contribution due to droplet deposition in Eq. (33) becomes more significant. This leads to the maxima observed towards the end of the pipe in Fig. 5(a) and (b).

5. Conclusion

In this paper, a model for interphase heat and mass transfer was presented and applied to forced convective boiling of binary mixtures in annular flow. The model is based on a Colburn–Drew type formulation and it incorporates hydrodynamic effects due to droplet interchange (as described in the first part of the paper) to the calculation of the interface heat flux.

The main conclusions arising from this study are as follows:

1. The process of droplet interchange coupled with the preferential evaporation of the more volatile component from the liquid film generate a local concentration imbalance between the liquid film and the entrained droplets. As a result, a difference in mean (saturation) temperature between the two liquid streams is observed.
2. The combined effect of mass transfer resistance (due to gradients of concentration building up adjacent to the interface in the gas core) and of droplet interchange give rise to interfacial temperatures higher than a mean temperature obtained via the calculation of the local enthalpy of the flow (mean equilibrium temperature). Therefore, increased wall temperatures are observed.
3. As far as the heat transfer coefficient is concerned, the deteriorating trends observed by Kandlbinder [1] at high qualities are well predicted by the present

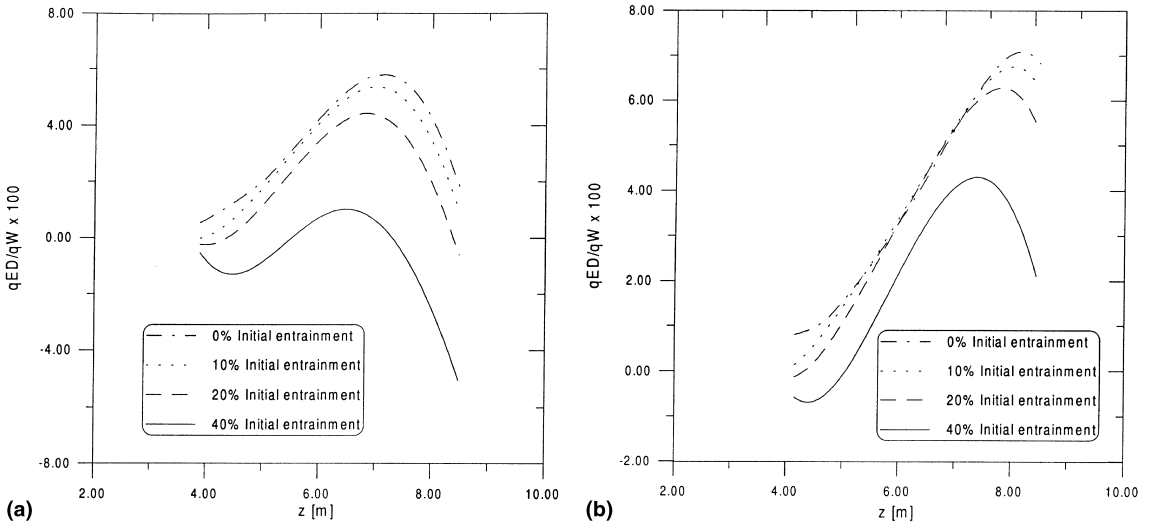

Fig. 5. Profiles of energy released/absorbed by entrained droplets: (a) Run 3, (b) Run 6. Conditions are those of Table 1.

formulation (α is defined as the ratio between the wall heat flux and the difference between the wall and the mean equilibrium temperatures). However, the accuracy of the predictions reduces with increasing pressure. This may be related to the fact that most of the correlations and methods used in the present formulation were devised based on low-pressure data.

Acknowledgements

The first author thanks the Brazilian National Research Council (CNPq – Conselho Nacional de Desenvolvimento Científico e Tecnológico) for the award of a scholarship (Grant No. 200085/97-2).

References

[1] T. Kandlbinder, Experimental investigation of forced convective boiling of hydrocarbons and hydrocarbon mixtures, Ph.D. thesis, University of London, Imperial College, 1997.
[2] J.C. Chen, A correlation for boiling heat transfer to saturated fluids in convective flow, ASME–AIChE Heat Transfer Conference, Boston, MA, 1963, Paper 63-HT-34.
[3] D.L. Bennett, J.C. Chen, Forced convective boiling in vertical tubes for saturated pure components and binary mixtures, AIChE J. 26 (3) (1980) 454–461.
[4] G.P. Celata, M. Cumo, T. Setaro, Forced convective boiling in binary mixtures, Int. J. Heat Mass Transfer 3 (13) (1993) 3299–3309.
[5] M.P. Mishra, H.K. Varma, C.P. Sharma, Heat transfer coefficients in forced convective evaporation of refrigerant mixtures, Lett. Heat Mass Transfer 8 (2) (1981) 127–136.
[6] J.W. Palen, Shell-and-tube reboilers: thermal design, in: G.F. Hewitt (Ed.), Handbook of Heat Exchanger Design, Begell House, New York, 1992, pp. 3.6.2-1–3.6.2-12.
[7] J.W. Palen, W.M. Small, A new way to design kettle and internal reboilers, Hydrocarbon Process. 43 (11) (1964) 199–208.
[8] S.G. Kandlikar, Boiling heat transfer with binary mixtures: Part II – flow boiling in plain tubes, J. Heat Transfer 120 (1998) 388–394.
[9] S.G. Kandlikar, A general correlation for saturated two-phase flow boiling heat transfer inside horizontal and vertical tubes, J. Heat Transfer 112 (1990) 219–228.
[10] L. Silver, Gas cooling with aqueous condensation, Trans. Inst. Chem. Eng. 25 (1947) 30–42.
[11] K.J. Bell, M.A. Ghaly, An approximate generalized design for multicomponent partial condensers, AIChE Symp. Ser. 69 (131) (1973) 72–79.
[12] J.W. Palen, C.C. Yang, J. Taborek, Application of the resistance proration method to boiling in tubes in the presence of inert gas, AIChE Symp. Ser. 76 (199) (1980) 282–288.
[13] R.G. Sardesai, R.A.W. Shock, D. Butterworth, Heat and mass transfer in multicomponent condensation and boiling, Heat Transfer Eng. 3 (3-4) (1982) 104–114.
[14] K. Murata, K. Hashizume, Forced convective boiling of nonazeotropic refrigerant mixtures inside tubes, J. Heat Transfer 115 (1993) 680–689.
[15] R.A.W. Shock, Evaporation of binary mixtures in upward annular flow, Int. J. Multiphase Flow 2 (1976) 411–433.
[16] G.F. Hewitt, Analysis of annular two-phase flow; application of the Duckler analysis to vertical upward flow in a tube, UKAEA Report AERE-3680, 1961.
[17] J.R. Thome, R.A.W. Shock, Boiling of multicomponent liquid mixtures, Adv. Heat Transfer 16 (1984) 59–156.
[18] D.R. Webb, J.M. McNaught, Condensers, Developments in Heat Exchanger Technology, 1980, Applied Science, Barking, UK.

[19] D.R. Webb, Condensation of vapour mixtures, in: G.F. Hewitt (Ed.), Handbook of Heat Exchanger Design, second ed., Begell House, New York, 1995, pp. 2.6.3-1–2.6.3-25.
[20] R.B. Bird, W.E. Stewart, E.N. Lightfoot, Transport Phenomena, Wiley, New York, 1960.
[21] D.R. Webb, M. Fahrner, R. Schwaab, The relationship between the Colburn and Silver methods for condenser design, Int. J. Heat Mass Transfer 39 (15) (1993) 3147–3156.
[22] E. Fuller, P.D. Schettler, J.C. Giddings, A new method for prediction of binary gas-phase diffusion coefficients, Indust. Eng. Chem. 58 (5) (1966) 19–23.